

RESEARCH ARTICLE

Prox-NAG-GS: A Semi-Implicit Proximal Method for Composite OptimizationSikeh Gisele Wiykiynyuy^a, Kelvin Asu Ekuri^a and Valentin Leplat^a^aInstitute of Data Science and Artificial Intelligence, Innopolis University**ARTICLE HISTORY**

Compiled May 27, 2026

ABSTRACT

Composite optimization problems, where a smooth loss is combined with a nonsmooth regularizer, are common in machine learning and inverse problems. In this work, we study a proximal extension of NAG-GS, a semi-implicit accelerated method obtained from a Gauss-Seidel discretization of an inertial dynamics. The proposed method, called Prox-NAG-GS, keeps the coupled structure of NAG-GS for the smooth part and replaces the second update by a proximal step. It therefore applies to objectives of the form $F = f + r$, where f is smooth and r is convex and proximable. We derive deterministic convergence guarantees for this method. The analysis has to account for a specific feature of the scheme. Prox-NAG-GS keeps two coupled sequences: an x -sequence, on which the gradient of the smooth term is evaluated, and a v -sequence, produced by the proximal update. The gradient is evaluated at x_{k+1} , whereas the proximal step returns v_{k+1} , which creates a mismatch absent from the standard proximal-gradient analysis. Under the sufficient condition that the proximal quadratic parameter is at least as large as the smoothness constant of f , we control this mismatch through an augmented Lyapunov function involving both sequences. This gives a linear convergence result in the strongly convex composite case. In the convex case, the same Lyapunov structure yields an $O(1/k)$ rate for the best iterate and for the averaged iterate. We test the method on deterministic Elastic Net and Group Lasso problems, and on stochastic sparse softmax-regression benchmarks. In the deterministic tests, Prox-NAG-GS reaches the same solutions as the baselines with substantially fewer iterations; for Group Lasso this also gives the best wall-clock time. In the stochastic tests, Prox-NAG-GS compares favorably with Prox-SGD in terms of data-fit reduction and gives similar test accuracies. The results also reveal a different regularization behavior: Prox-SGD usually produces sparser models and may give a lower full regularized objective when the nonsmooth regularization is large.

KEYWORDS

Composite optimization; proximal algorithms; semi-implicit methods; Lyapunov analysis; nonsmooth convex optimization; stochastic composite optimization

1. Introduction

Many optimization problems in machine learning, signal processing and inverse problems combine a smooth loss with a nonsmooth regularizer or constraint. A typical form is

$$\min_{x \in \mathbb{R}^d} F(x) := f(x) + r(x), \quad (1)$$

where f is differentiable and r is convex, possibly nonsmooth, but has an efficient proximal operator. This setting appears for instance in sparse regression, sparse logistic or softmax regression, Group Lasso, and constrained learning problems. In these examples, differentiating the regularizer is either impossible or not desirable. The usual approach is therefore to treat the smooth term by a gradient step and the nonsmooth term by a proximal step; see, e.g., [8, 24].

Proximal-gradient methods and their accelerated variants are among the standard algorithms for such problems. They are simple, robust, and well understood; classical examples include ISTA and FISTA [5], building on the acceleration ideas of Nesterov [20]. At the same time, accelerated and inertial methods can be sensitive to the way the underlying dynamics is discretized. This is one of the motivations behind NAG-GS [18], a semi-implicit method obtained from a Gauss-Seidel discretization of an accelerated continuous-time model. The method keeps two coupled variables and evaluates the gradient at the new x -iterate. This gives a different stability behavior compared with fully explicit momentum schemes.

The original NAG-GS method was designed for smooth objectives, or for settings where one can use a gradient-like oracle for the whole objective. In composite optimization, this is not the natural situation. Applying a gradient-type update directly to $F = f + r$ would ignore the structure of the nonsmooth term. Instead, the regularizer should be handled through its proximal operator. This motivates the question studied in this paper: can one combine the semi-implicit structure of NAG-GS with a proximal step for the nonsmooth part?

The construction is direct. The second update of NAG-GS can be interpreted as the minimizer of a quadratic model. Adding the nonsmooth term r to this quadratic model leads to a proximal update. The resulting method, which we call Prox-NAG-GS, reduces to NAG-GS when $r = 0$, and can be implemented with the same proximal maps used in classical splitting methods.

Our contributions are as follows.

- (i) We introduce Prox-NAG-GS, a proximal extension of NAG-GS [18] for composite objectives of the form (1).
- (ii) We prove deterministic convergence results for the proposed method. In the strongly convex composite case, we obtain a linear convergence rate under the conservative condition that the proximal quadratic parameter is at least as large as the smoothness constant of f . The proof relies on an augmented Lyapunov function involving both v_k and x_k . We also show that the same Lyapunov structure gives an $O(1/k)$ guarantee for the best iterate and for the averaged iterate in the convex case.
- (iii) We evaluate the method on deterministic Elastic Net and Group Lasso benchmarks, and compare it with ISTA, FISTA, and Chambolle-Pock.
- (iv) We also test stochastic sparse softmax regression with entrywise ℓ_1 and Group Lasso penalties. These experiments show that Prox-NAG-GS compares favorably with Prox-SGD in terms of data-fit reduction and gives similar test accuracies, while Prox-SGD usually produces sparser solutions.

The remainder of the paper is organized as follows. Section 1.1 reviews the most relevant proximal, inertial and accelerated methods for composite optimization. Section 2 introduces the composite problem and derives Prox-NAG-GS from the semi-implicit structure of NAG-GS. Section 3 presents the deterministic convergence analysis. We first establish the key one-step inequalities, then prove a linear convergence result in the strongly convex case, and finally derive an $O(1/k)$ guarantee in the convex case.

Section 4 reports numerical experiments on deterministic and stochastic composite optimization problems, with comparisons to standard proximal methods. Finally, Section 5 concludes and outlines future directions.

1.1. Related work

1.1.0.1. Proximal-gradient and splitting methods.. Problem (1) is the standard setting of proximal-gradient, or forward-backward, methods. These methods treat the smooth term f explicitly by a gradient step and the nonsmooth term r implicitly through its proximal operator. In the case of a least-squares loss with an ℓ_1 penalty, this gives ISTA [11]. More generally, forward-backward splitting is a basic tool for convex composite optimization; see, e.g., [4, 8, 9, 24]. Accelerated variants, in particular FISTA [5], are standard baselines for deterministic composite optimization. Related accelerated proximal-gradient schemes were also studied by Tseng [28] and Nesterov [21].

Other splitting methods are also relevant. Primal-dual methods, such as Chambolle-Pock [7] and Condat-Vũ type algorithms [10, 29], are especially useful when the nonsmooth term is composed with a linear operator or when constraints are better handled through a saddle-point formulation. In our numerical experiments, we include Chambolle-Pock as one of the deterministic baselines.

1.1.0.2. Stochastic composite optimization.. In large-scale learning, the smooth term often has the finite-sum form

$$f(x) = \frac{1}{n} \sum_{i=1}^n f_i(x),$$

and gradients are computed from mini-batches. This has motivated stochastic proximal and stochastic composite-gradient methods. Early examples include FOBOS [13] and regularized dual averaging [31]. Stochastic approximation methods for composite objectives were further developed in, for example, [14, 15, 17]; see also the survey [6] for a broader discussion of stochastic optimization.

For finite-sum problems, variance-reduced methods such as SVRG, Prox-SVRG, SAG, and SAGA are also important references [12, 16, 26, 32]. They are not the main focus of this paper. In the stochastic experiments, we use Prox-SGD as a first baseline, because it is the direct stochastic counterpart of proximal-gradient descent and uses the proximal operator at every stochastic step.

1.1.0.3. Acceleration, inertial dynamics, and NAG-GS.. Acceleration can be studied from the discrete viewpoint, as in Nesterov’s accelerated gradient method [20, 22], or through continuous-time inertial dynamics. The continuous-time point of view has led to a better understanding of accelerated methods and their Lyapunov functions; see, e.g., [3, 27, 30]. There is also a large literature on inertial proximal and inertial forward-backward methods, going back to the heavy-ball method [25] and including splitting schemes such as [2, 19, 23].

NAG-GS [18] belongs to this line of work, but uses a semi-implicit Gauss-Seidel discretization of an accelerated dynamics. The present paper studies a proximal extension of this idea. The resulting method is close in spirit to forward-backward splitting, but the NAG-GS coupling changes the analysis: the gradient is evaluated at x_{k+1} , while

the proximal step produces v_{k+1} . This mismatch is the main point handled in the convergence proof.

2. Composite problem and Prox-NAG-GS

2.1. Problem class

We consider the composite optimization problem

$$\min_{x \in \mathbb{R}^d} F(x) := f(x) + r(x), \quad (2)$$

where $f : \mathbb{R}^d \rightarrow \mathbb{R}$ is differentiable, and $r : \mathbb{R}^d \rightarrow \mathbb{R} \cup \{+\infty\}$ is proper, closed and convex. We assume that r is proximal, in the sense that, for every $\lambda > 0$, the proximal operator

$$\text{prox}_{\lambda r}(z) := \operatorname{argmin}_{u \in \mathbb{R}^d} \left\{ r(u) + \frac{1}{2\lambda} \|u - z\|^2 \right\} \quad (3)$$

can be computed efficiently. This framework also covers simple convex constraints, by taking r to be the indicator function of a closed convex set, in which case the proximal operator is the Euclidean projection.

Two examples will be used in the numerical section. For the ℓ_1 penalty $r(x) = \lambda_1 \|x\|_1$, the proximal operator is the soft-thresholding map. For the Group Lasso penalty

$$r(x) = \lambda_g \sum_{G \in \mathcal{G}} \|x_G\|_2,$$

the proximal operator is block separable and, on each group, is given by

$$\text{prox}_{\tau \lambda_g \|\cdot\|_2}(x_G) = \left(1 - \frac{\tau \lambda_g}{\|x_G\|_2} \right)_+ x_G, \quad (4)$$

with the usual convention that the right-hand side is zero when $x_G = 0$.

For the deterministic analysis, we will use the following assumptions. The first one corresponds to the convex case, while the second one will be added for the linear convergence result.

Assumption 1 (Convex composite setting). The function f is convex, differentiable and L -smooth. The function r is proper, closed and convex. The composite function $F = f + r$ admits a minimizer x^* .

Assumption 2 (Strongly convex composite setting). Assumption 1 holds. Moreover, f is μ_f -strongly convex, and $F = f + r$ is μ_F -strongly convex.

Since r is convex, one can take $\mu_F = \mu_f$ when f is μ_f -strongly convex. We keep the two constants in the notation because the proof only uses strong convexity of f in one place, and strong convexity of F in another.

We also distinguish these curvature constants from the algorithmic parameter $\hat{\mu}$ used in Prox-NAG-GS. This distinction is important. The parameter $\hat{\mu}$ controls the

quadratic term in the proximal subproblem. In the convergence analysis, we will impose the sufficient condition $\widehat{\mu} \geq L$. This condition is conservative, but it gives a regime in which the proximal quadratic model is strong enough to control the mismatch created by the semi-implicit update. In the numerical experiments, $\widehat{\mu}$ is treated as a tunable parameter.

2.2. From NAG-GS to a proximal update

The smooth NAG-GS method uses two variables, x_k and v_k . Given a step parameter $\alpha_k > 0$, we define

$$a_k = \frac{\alpha_k}{1 + \alpha_k}.$$

The first update is

$$x_{k+1} = (1 - a_k)x_k + a_kv_k. \quad (5)$$

The second update can be written as a gradient step from an intermediate point. Let

$$z_{k+1} := (1 - b_k)v_k + b_kx_{k+1},$$

where $b_k \in (0, 1)$ is defined below. In the smooth case, the update

$$v_{k+1} = z_{k+1} - \frac{b_k}{\widehat{\mu}}g_{k+1}$$

is equivalently the minimizer of the quadratic model

$$v \mapsto \langle g_{k+1}, v \rangle + \frac{\widehat{\mu}}{2b_k} \|v - z_{k+1}\|^2.$$

Here g_{k+1} is a gradient, or a gradient estimator, of the smooth part at x_{k+1} .

This form makes the proximal extension immediate. We add the nonsmooth term $r(v)$ to the quadratic model. This gives

$$v_{k+1} = \text{prox}_{\frac{b_k}{\widehat{\mu}}r} \left(z_{k+1} - \frac{b_k}{\widehat{\mu}}g_{k+1} \right). \quad (6)$$

When $r = 0$, this reduces to the smooth NAG-GS update.

2.3. The algorithm

The resulting method is given in Algorithm 1. In the deterministic case, we use $g_{k+1} = \nabla f(x_{k+1})$. In the stochastic case, g_{k+1} is computed from a mini-batch. The convergence analysis in Section 3 is deterministic; the stochastic variant is studied numerically in Section 4.

The method is close in spirit to forward-backward splitting, since the smooth part is treated by a gradient step and the nonsmooth part by a proximal step. The difference is that the gradient is evaluated at the new point x_{k+1} , which is coupled with v_k ,

Algorithm 1 Prox-NAG-GS for composite optimization

Require: $x_0 \in \mathbb{R}^d$, $v_0 = x_0$, parameters $\widehat{\mu} > 0$, $\gamma_0 > 0$, step parameters $\alpha_k > 0$, proximal operator $\text{prox}_{\lambda r}$

- 1: **for** $k = 0, 1, 2, \dots$ **do**
- 2: $a_k \leftarrow \alpha_k / (1 + \alpha_k)$
- 3: $x_{k+1} \leftarrow (1 - a_k)x_k + a_k v_k$
- 4: $b_k \leftarrow \alpha_k \widehat{\mu} / (\alpha_k \widehat{\mu} + \gamma_k)$
- 5: $z_{k+1} \leftarrow (1 - b_k)v_k + b_k x_{k+1}$
- 6: compute g_{k+1} , a gradient or stochastic gradient of f at x_{k+1}
- 7:

$$v_{k+1} \leftarrow \text{prox}_{\frac{b_k}{\widehat{\mu}} r} \left(z_{k+1} - \frac{b_k}{\widehat{\mu}} g_{k+1} \right)$$

- 8: $\gamma_{k+1} \leftarrow (1 - a_k)\gamma_k + a_k \widehat{\mu}$
 - 9: **end for**
-

while the proximal step produces v_{k+1} . This is the semi-implicit structure inherited from NAG-GS. It is also the main point that has to be handled in the convergence analysis.

3. Convergence analysis

In this section, we study Prox-NAG-GS in the deterministic composite setting. The analysis has two parts. We first derive estimates that are valid under the convex composite setting of Assumption 1. We then use these estimates in two different ways. Under the strongly convex setting of Assumption 2, we prove a linear convergence result. In the merely convex case, we prove an $O(1/k)$ guarantee for the best iterate and for the averaged iterate.

The analysis is not a direct application of the standard proximal-gradient proof. The difficulty comes from the point at which the gradient is evaluated. The proximal step returns v_{k+1} , while the gradient of the smooth part is evaluated at x_{k+1} . Hence the optimality condition of the proximal subproblem does not directly give an element of $\partial F(v_{k+1})$. This produces a mismatch term that has to be controlled.

The proof is organized as follows. We first fix a constant-parameter regime and derive the proximal identities, the geometric identities, and the main one-step inequality. These estimates are common to both convergence results. The mismatch term is then absorbed under the sufficient condition $\widehat{\mu} \geq L$. For the strongly convex case, a natural Lyapunov candidate does not close, and one has to add a term involving $\|x_k - x^*\|^2$. This gives a linear convergence result. Finally, we show that the same augmented energy also gives a descent inequality in the convex case.

Throughout this section, x^* denotes a minimizer of $F = f + r$, and

$$F^* := F(x^*).$$

Unless stated otherwise, Assumption 1 is in force. The additional strong convexity assumptions are only used in the subsection devoted to the linear convergence result.

3.1. Constant-parameter regime

We focus on the constant-damping regime

$$\gamma_0 = \widehat{\mu}.$$

Then the recursion for γ_k gives $\gamma_k \equiv \widehat{\mu}$, and therefore

$$b_k = a_k = \frac{\alpha_k}{1 + \alpha_k}.$$

In the convergence results below, we further assume that a_k is constant:

$$a_k \equiv a \in (0, 1).$$

The deterministic Prox-NAG-GS iteration then reads

$$\begin{aligned} x_{k+1} &= (1 - a)x_k + av_k, \\ z_{k+1} &= (1 - a)v_k + ax_{k+1}, \\ v_{k+1} &= \text{prox}_{\frac{a}{\widehat{\mu}}r} \left(z_{k+1} - \frac{a}{\widehat{\mu}} \nabla f(x_{k+1}) \right). \end{aligned} \tag{7}$$

The parameter $\widehat{\mu}$ is an algorithmic curvature parameter. It is not necessarily equal to the strong convexity constant of f . In the proof below, we will require $\widehat{\mu} \geq L$. This is a sufficient condition ensuring that the quadratic model used in the proximal step is strong enough to compensate for the smoothness error of f .

3.2. Proximal identities

We first collect two standard consequences of the proximal update.

Lemma 1 (Optimality condition). *Let v_{k+1} be generated by (7). Then v_{k+1} is the unique minimizer of*

$$v \mapsto r(v) + \langle \nabla f(x_{k+1}), v \rangle + \frac{\widehat{\mu}}{2a} \|v - z_{k+1}\|^2.$$

Moreover, there exists $s_{k+1} \in \partial r(v_{k+1})$ such that

$$0 = s_{k+1} + \nabla f(x_{k+1}) + \frac{\widehat{\mu}}{a} (v_{k+1} - z_{k+1}). \tag{8}$$

Equivalently, if

$$q_{k+1} := \frac{\widehat{\mu}}{a} (z_{k+1} - v_{k+1}), \tag{9}$$

then

$$q_{k+1} = \nabla f(x_{k+1}) + s_{k+1}. \tag{10}$$

Proof. By definition of the proximal operator, v_{k+1} minimizes

$$r(v) + \frac{\widehat{\mu}}{2a} \left\| v - \left(z_{k+1} - \frac{a}{\widehat{\mu}} \nabla f(x_{k+1}) \right) \right\|^2.$$

Expanding the square and removing the terms independent of v gives the stated minimization problem. Since r is convex and the quadratic term is strongly convex, this minimizer is unique. The optimality condition gives (8), and (10) follows by rearranging the terms. \square

Lemma 2 (Three-point inequality). *For every $u \in \mathbb{R}^d$, the iterate v_{k+1} satisfies*

$$\begin{aligned} & r(v_{k+1}) + \langle \nabla f(x_{k+1}), v_{k+1} \rangle + \frac{\widehat{\mu}}{2a} \|v_{k+1} - z_{k+1}\|^2 \\ & \leq r(u) + \langle \nabla f(x_{k+1}), u \rangle + \frac{\widehat{\mu}}{2a} \|u - z_{k+1}\|^2 - \frac{\widehat{\mu}}{2a} \|u - v_{k+1}\|^2. \end{aligned} \quad (11)$$

Proof. The function minimized in Lemma 1 is $\widehat{\mu}/a$ -strongly convex and is minimized at v_{k+1} . Therefore, for every u ,

$$\phi_k(u) \geq \phi_k(v_{k+1}) + \frac{\widehat{\mu}}{2a} \|u - v_{k+1}\|^2,$$

where

$$\phi_k(v) = r(v) + \langle \nabla f(x_{k+1}), v \rangle + \frac{\widehat{\mu}}{2a} \|v - z_{k+1}\|^2.$$

Rearranging gives (11). \square

The next observation explains where the proof differs from the standard proximal-gradient analysis. By Lemma 1,

$$q_{k+1} = \nabla f(x_{k+1}) + s_{k+1}, \quad s_{k+1} \in \partial r(v_{k+1}).$$

If the gradient were evaluated at v_{k+1} , then q_{k+1} would be an element of $\partial F(v_{k+1})$. Here, instead,

$$q_{k+1} = \underbrace{\nabla f(v_{k+1}) + s_{k+1}}_{\in \partial F(v_{k+1})} + \underbrace{\nabla f(x_{k+1}) - \nabla f(v_{k+1})}_{\text{mismatch}}.$$

The L -smoothness of f gives

$$\|\nabla f(x_{k+1}) - \nabla f(v_{k+1})\| \leq L \|x_{k+1} - v_{k+1}\|.$$

Thus the quantity $\|x_{k+1} - v_{k+1}\|^2$ will appear in the proof.

3.3. Geometric identities

We now record the identities coming only from the two affine updates in (7).

Lemma 3 (Kinematic identities). *For every k ,*

$$x_{k+1} - v_k = (1 - a)(x_k - v_k), \quad (12)$$

$$x_{k+1} - z_{k+1} = (1 - a)^2(x_k - v_k), \quad (13)$$

and

$$x_{k+1} - v_{k+1} = (1 - a)^2(x_k - v_k) + (z_{k+1} - v_{k+1}). \quad (14)$$

Proof. The first identity follows directly from

$$x_{k+1} = (1 - a)x_k + av_k.$$

Since

$$z_{k+1} = (1 - a)v_k + ax_{k+1},$$

we also have

$$x_{k+1} - z_{k+1} = (1 - a)(x_{k+1} - v_k),$$

which gives (13). The last identity follows by writing

$$x_{k+1} - v_{k+1} = (x_{k+1} - z_{k+1}) + (z_{k+1} - v_{k+1}).$$

□

We shall also use the following identity for the distance of x_k to the solution.

Lemma 4 (Recursion for x_k). *Let*

$$X_k := \|x_k - x^*\|^2, \quad V_k := \|v_k - x^*\|^2, \quad D_k := \|x_k - v_k\|^2.$$

Then

$$X_{k+1} = (1 - a)X_k + aV_k - a(1 - a)D_k. \quad (15)$$

Proof. Since $x_{k+1} = (1 - a)x_k + av_k$, we have

$$x_{k+1} - x^* = (1 - a)(x_k - x^*) + a(v_k - x^*).$$

Using the identity

$$\|(1 - a)p + aq\|^2 = (1 - a)\|p\|^2 + a\|q\|^2 - a(1 - a)\|p - q\|^2$$

gives (15). □

3.4. A one-step inequality

We now combine the three-point inequality with the smoothness of f . The estimate below is written with a parameter $\mu_f \geq 0$ such that f is μ_f -strongly convex. In the merely convex case, we simply take $\mu_f = 0$. When the strongly convex setting is considered, μ_f is the strong convexity constant of f .

Proposition 1 (One-step inequality). *Let $(x_{k+1}, z_{k+1}, v_{k+1})$ be generated by (7). Assume that f is L -smooth and μ_f -strongly convex, with the convention $\mu_f = 0$ in the merely convex case. Then, for every $u \in \mathbb{R}^d$,*

$$F(v_{k+1}) - F(u) \leq \frac{\hat{\mu}}{2a} \left(\|u - z_{k+1}\|^2 - \|u - v_{k+1}\|^2 - \|v_{k+1} - z_{k+1}\|^2 \right) - \frac{\mu_f}{2} \|u - x_{k+1}\|^2 + \frac{L}{2} \|v_{k+1} - x_{k+1}\|^2. \quad (16)$$

Proof. By L -smoothness of f ,

$$f(v_{k+1}) \leq f(x_{k+1}) + \langle \nabla f(x_{k+1}), v_{k+1} - x_{k+1} \rangle + \frac{L}{2} \|v_{k+1} - x_{k+1}\|^2.$$

Adding this inequality to (11) gives

$$\begin{aligned} F(v_{k+1}) &\leq f(x_{k+1}) + \langle \nabla f(x_{k+1}), u - x_{k+1} \rangle + r(u) \\ &\quad + \frac{\hat{\mu}}{2a} \|u - z_{k+1}\|^2 - \frac{\hat{\mu}}{2a} \|u - v_{k+1}\|^2 - \frac{\hat{\mu}}{2a} \|v_{k+1} - z_{k+1}\|^2 \\ &\quad + \frac{L}{2} \|v_{k+1} - x_{k+1}\|^2. \end{aligned}$$

Using the μ_f -strong convexity of f ,

$$f(x_{k+1}) + \langle \nabla f(x_{k+1}), u - x_{k+1} \rangle \leq f(u) - \frac{\mu_f}{2} \|u - x_{k+1}\|^2.$$

Substitution gives the result. \square

We next apply Proposition 1 with $u = x^*$. The only point to expand is the term $\|x^* - z_{k+1}\|^2$.

Lemma 5 (Expansion at the solution). *Let*

$$G_k := F(v_k) - F^*, \quad V_k := \|v_k - x^*\|^2, \quad X_k := \|x_k - x^*\|^2,$$

and

$$D_k := \|x_k - v_k\|^2, \quad R_{k+1} := \|v_{k+1} - z_{k+1}\|^2, \quad M_{k+1} := \|v_{k+1} - x_{k+1}\|^2.$$

Then

$$\begin{aligned} G_{k+1} + \frac{\hat{\mu}}{2a} V_{k+1} &\leq \frac{\hat{\mu}(1-a)}{2a} V_k + \frac{\hat{\mu} - \mu_f}{2} X_{k+1} \\ &\quad - \frac{\hat{\mu}(1-a)^3}{2} D_k - \frac{\hat{\mu}}{2a} R_{k+1} + \frac{L}{2} M_{k+1}. \end{aligned} \quad (17)$$

Proof. Applying Proposition 1 with $u = x^*$ gives

$$G_{k+1} + \frac{\hat{\mu}}{2a} V_{k+1} \leq \frac{\hat{\mu}}{2a} \|x^* - z_{k+1}\|^2 - \frac{\mu_f}{2} X_{k+1} - \frac{\hat{\mu}}{2a} R_{k+1} + \frac{L}{2} M_{k+1}.$$

Since

$$z_{k+1} = (1 - a)v_k + ax_{k+1},$$

we have

$$\|x^* - z_{k+1}\|^2 = (1 - a)V_k + aX_{k+1} - a(1 - a) \|x_{k+1} - v_k\|^2.$$

By Lemma 3,

$$\|x_{k+1} - v_k\|^2 = (1 - a)^2 D_k.$$

Substituting these two identities gives (17). □

3.5. Why the first Lyapunov candidate does not close

Let us explain the main difficulty before proving the final contraction. A first natural candidate is

$$G_k + \frac{\hat{\mu}}{2a} V_k.$$

This is the expected energy if one tries to imitate a standard strongly convex proximal analysis. However, Lemma 5 contains the additional term

$$\frac{L}{2} M_{k+1} = \frac{L}{2} \|v_{k+1} - x_{k+1}\|^2.$$

This term comes from the mismatch between the gradient point x_{k+1} and the proximal point v_{k+1} .

If one takes the natural choice $\hat{\mu} = \mu_f$, the term involving X_{k+1} disappears from (17). But the mismatch term remains, and it cannot be absorbed in general unless the proximal quadratic model is strong enough compared with the smoothness of f . This is why we impose the sufficient condition

$$\hat{\mu} \geq L.$$

This condition allows us to absorb the mismatch term. The price to pay is that, in general, $\hat{\mu} > \mu_f$, and therefore the positive term

$$\frac{\hat{\mu} - \mu_f}{2} X_{k+1}$$

appears in (17). The identity (15) then shows how to handle it: we add a multiple of $X_k = \|x_k - x^*\|^2$ to the Lyapunov function.

This gives the augmented Lyapunov function

$$\mathcal{L}_k = G_k + bV_k + cX_k,$$

with suitable constants $b > 0$ and $c > 0$.

3.6. Absorbing the mismatch term

We now show that $\hat{\mu} \geq L$ is sufficient to remove the mismatch term from the one-step inequality.

Lemma 6 (Absorption of the mismatch term). *Assume that $\hat{\mu} \geq L$. Then*

$$-\frac{\hat{\mu}(1-a)^3}{2}D_k - \frac{\hat{\mu}}{2a}R_{k+1} + \frac{L}{2}M_{k+1} \leq 0. \quad (18)$$

Proof. By Lemma 3,

$$x_{k+1} - v_{k+1} = (1-a)^2(x_k - v_k) + (z_{k+1} - v_{k+1}).$$

Using Young's inequality in the form

$$\|p + q\|^2 \leq \frac{1}{1-a} \|p\|^2 + \frac{1}{a} \|q\|^2,$$

with

$$p = (1-a)^2(x_k - v_k), \quad q = z_{k+1} - v_{k+1},$$

we obtain

$$M_{k+1} \leq (1-a)^3 D_k + \frac{1}{a} R_{k+1}.$$

Therefore,

$$\begin{aligned} & -\frac{\hat{\mu}(1-a)^3}{2}D_k - \frac{\hat{\mu}}{2a}R_{k+1} + \frac{L}{2}M_{k+1} \\ & \leq -\frac{\hat{\mu}-L}{2}(1-a)^3 D_k - \frac{\hat{\mu}-L}{2a}R_{k+1}. \end{aligned}$$

The right-hand side is nonpositive because $\hat{\mu} \geq L$. □

Combining Lemma 5 and Lemma 6 gives the following simplified estimate.

Proposition 2 (Reduced one-step inequality). *Assume that $\hat{\mu} \geq L$. Then*

$$G_{k+1} + \frac{\hat{\mu}}{2a}V_{k+1} \leq \frac{\hat{\mu}(1-a)}{2a}V_k + \frac{\hat{\mu}-\mu_f}{2}X_{k+1}. \quad (19)$$

Proof. This follows directly from Lemma 5 and Lemma 6. □

3.7. Strongly convex case: augmented Lyapunov function

We now prove the contraction of the augmented Lyapunov function. Define

$$b := \frac{\widehat{\mu}}{2a}, \quad \beta := \frac{\widehat{\mu} - \mu_f}{2}. \quad (20)$$

With this notation, Proposition 2 becomes

$$G_{k+1} + bV_{k+1} \leq b(1-a)V_k + \beta X_{k+1}. \quad (21)$$

Let $c > 0$, to be chosen below, and define

$$\mathcal{L}_k := G_k + bV_k + cX_k. \quad (22)$$

Lemma 7 (Lyapunov contraction). *Assume that Assumption 2 holds and that $\widehat{\mu} \geq L$. Let b and β be defined by (20). Choose $c > 0$ such that*

$$\frac{\beta(1-a)}{a} < c < \frac{\widehat{\mu} + \mu_F}{2a} - \beta. \quad (23)$$

Then

$$\mathcal{L}_{k+1} \leq \theta \mathcal{L}_k, \quad \forall k \geq 0,$$

where

$$\theta := \max \left\{ \frac{b(1-a) + a(\beta + c)}{b + \mu_F/2}, \frac{(1-a)(\beta + c)}{c} \right\}. \quad (24)$$

Moreover, $\theta < 1$.

Proof. Adding cX_{k+1} to (21) gives

$$\mathcal{L}_{k+1} \leq b(1-a)V_k + (\beta + c)X_{k+1}.$$

Using the identity (15), we get

$$\mathcal{L}_{k+1} \leq b(1-a)V_k + (\beta + c)((1-a)X_k + aV_k - a(1-a)D_k).$$

Since $\widehat{\mu} \geq L \geq \mu_f$, we have $\beta \geq 0$. Hence $-a(1-a)(\beta + c)D_k \leq 0$, and dropping this term gives

$$\mathcal{L}_{k+1} \leq [b(1-a) + a(\beta + c)]V_k + (1-a)(\beta + c)X_k. \quad (25)$$

Since F is μ_F -strongly convex and x^* minimizes F ,

$$G_k = F(v_k) - F^* \geq \frac{\mu_F}{2}V_k.$$

Hence

$$\mathcal{L}_k = G_k + bV_k + cX_k \geq \left(b + \frac{\mu_F}{2}\right)V_k + cX_k.$$

Therefore, $\mathcal{L}_{k+1} \leq \theta \mathcal{L}_k$ holds with θ defined in (24).

It remains to check that $\theta < 1$. The second ratio in (24) is smaller than one if and only if

$$(1 - a)(\beta + c) < c,$$

which is equivalent to

$$c > \frac{\beta(1 - a)}{a}.$$

The first ratio is smaller than one if and only if

$$b(1 - a) + a(\beta + c) < b + \frac{\mu_F}{2}.$$

Since $b = \widehat{\mu}/(2a)$, this is equivalent to

$$c < \frac{\widehat{\mu} + \mu_F}{2a} - \beta.$$

These are exactly the two inequalities in (23).

Finally, the interval in (23) is nonempty. Indeed,

$$\begin{aligned} \left(\frac{\widehat{\mu} + \mu_F}{2a} - \beta\right) - \frac{\beta(1 - a)}{a} &= \frac{1}{a} \left(\frac{\widehat{\mu} + \mu_F}{2} - \beta\right) \\ &= \frac{1}{a} \left(\frac{\widehat{\mu} + \mu_F}{2} - \frac{\widehat{\mu} - \mu_f}{2}\right) \\ &= \frac{\mu_F + \mu_f}{2a} > 0. \end{aligned}$$

Thus such a c exists, and for any such choice we have $\theta < 1$. □

We can now state the convergence theorem.

Theorem 1 (Linear convergence). *Assume that Assumption 2 holds. Assume also that Prox-NAG-GS is run in the constant-parameter regime*

$$x_{k+1} = (1 - a)x_k + av_k, \quad z_{k+1} = (1 - a)v_k + ax_{k+1},$$

$$v_{k+1} = \text{prox}_{\frac{a}{\widehat{\mu}}r} \left(z_{k+1} - \frac{a}{\widehat{\mu}} \nabla f(x_{k+1}) \right),$$

with $a \in (0, 1)$. Finally, assume that the algorithmic curvature parameter satisfies

$$\widehat{\mu} \geq L.$$

Let

$$b := \frac{\hat{\mu}}{2a}, \quad \beta := \frac{\hat{\mu} - \mu_f}{2},$$

and choose any

$$c \in \left(\frac{\beta(1-a)}{a}, \frac{\hat{\mu} + \mu_F}{2a} - \beta \right).$$

Define

$$\mathcal{L}_k := F(v_k) - F^* + b \|v_k - x^*\|^2 + c \|x_k - x^*\|^2.$$

Then

$$\mathcal{L}_{k+1} \leq \theta \mathcal{L}_k, \quad \forall k \geq 0,$$

where

$$\theta := \max \left\{ \frac{b(1-a) + a(\beta+c)}{b + \mu_F/2}, \frac{(1-a)(\beta+c)}{c} \right\} < 1.$$

Consequently, for every $k \geq 0$,

$$F(v_k) - F^* \leq \mathcal{L}_0 \theta^k,$$

and

$$\|v_k - x^*\|^2 \leq \frac{\mathcal{L}_0}{b} \theta^k, \quad \|x_k - x^*\|^2 \leq \frac{\mathcal{L}_0}{c} \theta^k.$$

Proof. The contraction

$$\mathcal{L}_{k+1} \leq \theta \mathcal{L}_k$$

is exactly Lemma 7. Iterating it gives

$$\mathcal{L}_k \leq \theta^k \mathcal{L}_0.$$

Since

$$F(v_k) - F^* \leq \mathcal{L}_k, \quad b \|v_k - x^*\|^2 \leq \mathcal{L}_k, \quad c \|x_k - x^*\|^2 \leq \mathcal{L}_k,$$

the three estimates follow. \square

Remark 1 (Role of the condition $\hat{\mu} \geq L$). The condition $\hat{\mu} \geq L$ is sufficient, not necessary. It means that the quadratic term in the proximal subproblem is strong enough to dominate the smoothness error caused by the mismatch between x_{k+1} and v_{k+1} . Equivalently, the effective proximal-gradient stepsize $a/\hat{\mu}$ is at most a/L .

This condition is conservative. In the numerical experiments, the parameters are tuned empirically, and the best values can be more aggressive than those covered by

the theorem. The theorem should therefore be read as a stability and convergence guarantee for Prox-NAG-GS, not as a complete description of all parameter regimes that work in practice.

Remark 2 (On the rate). The theorem proves a linear rate, but we do not claim that the contraction factor θ is optimal. For strongly convex composite problems, accelerated proximal-gradient methods can achieve sharper worst-case rates. The contribution here is different: we prove that the semi-implicit proximal coupling used by Prox-NAG-GS admits a Lyapunov function and converges linearly in a well-defined deterministic regime.

Remark 3 (Why the additional X_k term is needed). The term $cX_k = c\|x_k - x^*\|^2$ is not added for cosmetic reasons. After absorbing the mismatch term with $\widehat{\mu} \geq L$, the one-step inequality still contains the positive term βX_{k+1} , where $\beta = (\widehat{\mu} - \mu_f)/2$. The identity

$$X_{k+1} = (1 - a)X_k + aV_k - a(1 - a)D_k$$

allows this term to be propagated through the Lyapunov function. This is the reason for using the augmented energy

$$\mathcal{L}_k = F(v_k) - F^* + b\|v_k - x^*\|^2 + c\|x_k - x^*\|^2.$$

Remark 4 (Smooth case). When $r = 0$, the proximal operator becomes the identity map, and Prox-NAG-GS reduces to the corresponding smooth semi-implicit NAG-GS update in the constant-parameter regime considered in this section. Therefore, Theorem 1 also gives a linear convergence result for this smooth specialization, provided that $\widehat{\mu} \geq L$.

This should not be confused with an optimal accelerated rate, nor with a complete analysis of all NAG-GS parameter regimes. It gives a conservative but rigorous linear-convergence regime for the smooth semi-implicit update.

3.8. Convex case: best-iterate and averaged rates

We now record what the same analysis gives in the merely convex case. This result is not needed for the linear convergence theorem above, but it is useful to complete the theoretical picture. It shows that the augmented Lyapunov function is not specific to strong convexity: the additional term $\|x_k - x^*\|^2$ is already the right quantity to obtain a descent estimate when $F = f + r$ is convex.

In this subsection, we assume that f is convex and L -smooth, that r is proper, closed, convex and proximal, and that $F = f + r$ admits a minimizer x^* . We keep the same constant-parameter regime as in the previous subsections, with $a \in (0, 1)$, and we assume

$$\widehat{\mu} \geq L.$$

Under this condition, the mismatch term between the gradient point x_{k+1} and the proximal point v_{k+1} can be absorbed as before. We then obtain a descent inequality for the same type of augmented Lyapunov function. As a consequence, the method satisfies an $O(1/k)$ rate for the best iterate and for the averaged iterate.

Theorem 2 (Convex case). *Assume that Assumption 1 holds. Assume also that Prox-NAG-GS is run in the constant-parameter regime*

$$x_{k+1} = (1 - a)x_k + av_k, \quad z_{k+1} = (1 - a)v_k + ax_{k+1},$$

$$v_{k+1} = \text{prox}_{\frac{a}{\hat{\mu}}r} \left(z_{k+1} - \frac{a}{\hat{\mu}} \nabla f(x_{k+1}) \right),$$

with $a \in (0, 1)$. Finally, assume that the algorithmic curvature parameter satisfies

$$\hat{\mu} \geq L.$$

Let

$$G_k := F(v_k) - F^*, \quad V_k := \|v_k - x^*\|^2, \quad X_k := \|x_k - x^*\|^2,$$

and define

$$\mathcal{E}_k := G_k + \frac{\hat{\mu}}{2a} V_k + \frac{\hat{\mu}(1-a)}{2a} X_k.$$

Then, for every $k \geq 0$,

$$\mathcal{E}_{k+1} \leq \mathcal{E}_k - G_k - \frac{\hat{\mu}(1-a)}{2} \|x_k - v_k\|^2. \quad (26)$$

Consequently,

$$\sum_{i=0}^{k-1} (F(v_i) - F^*) \leq \mathcal{E}_0, \quad k \geq 1, \quad (27)$$

and

$$\sum_{i=0}^{k-1} \|x_i - v_i\|^2 \leq \frac{2\mathcal{E}_0}{\hat{\mu}(1-a)}. \quad (28)$$

In particular,

$$\min_{0 \leq i \leq k-1} (F(v_i) - F^*) \leq \frac{\mathcal{E}_0}{k}. \quad (29)$$

Moreover, if

$$\bar{v}_k := \frac{1}{k} \sum_{i=0}^{k-1} v_i,$$

then

$$F(\bar{v}_k) - F^* \leq \frac{\mathcal{E}_0}{k}. \quad (30)$$

Finally,

$$F(v_k) \rightarrow F^*.$$

Proof. Since f is only assumed convex in this subsection, we use the reduced one-step inequality with $\mu_f = 0$. From Proposition 2, and since $\hat{\mu} \geq L$, we have

$$G_{k+1} + \frac{\hat{\mu}}{2a} V_{k+1} \leq \frac{\hat{\mu}(1-a)}{2a} V_k + \frac{\hat{\mu}}{2} X_{k+1}. \quad (31)$$

Set

$$b := \frac{\hat{\mu}}{2a}, \quad c := \frac{\hat{\mu}(1-a)}{2a} = b(1-a).$$

Then $\hat{\mu}/2 = ab$, and (31) becomes

$$G_{k+1} + bV_{k+1} \leq b(1-a)V_k + abX_{k+1}.$$

Adding cX_{k+1} to both sides gives

$$\mathcal{E}_{k+1} \leq b(1-a)V_k + (ab+c)X_{k+1}.$$

Since $c = b(1-a)$, we have

$$ab + c = ab + b(1-a) = b.$$

Therefore,

$$\mathcal{E}_{k+1} \leq b(1-a)V_k + bX_{k+1}. \quad (32)$$

We now use the identity

$$X_{k+1} = (1-a)X_k + aV_k - a(1-a)\|x_k - v_k\|^2.$$

Substituting this identity into (32), we obtain

$$\begin{aligned} \mathcal{E}_{k+1} &\leq b(1-a)V_k + b \left((1-a)X_k + aV_k - a(1-a)\|x_k - v_k\|^2 \right) \\ &= bV_k + b(1-a)X_k - ab(1-a)\|x_k - v_k\|^2. \end{aligned}$$

Using $c = b(1-a)$ and $ab = \hat{\mu}/2$, this becomes

$$\mathcal{E}_{k+1} \leq bV_k + cX_k - \frac{\hat{\mu}(1-a)}{2}\|x_k - v_k\|^2.$$

Since

$$\mathcal{E}_k = G_k + bV_k + cX_k,$$

we obtain

$$\mathcal{E}_{k+1} \leq \mathcal{E}_k - G_k - \frac{\widehat{\mu}(1-a)}{2} \|x_k - v_k\|^2,$$

which proves (26).

Summing (26) from $i = 0$ to $k - 1$ gives

$$\mathcal{E}_k + \sum_{i=0}^{k-1} G_i + \frac{\widehat{\mu}(1-a)}{2} \sum_{i=0}^{k-1} \|x_i - v_i\|^2 \leq \mathcal{E}_0.$$

Since $\mathcal{E}_k \geq 0$, this implies (27) and (28). The best-iterate estimate follows immediately:

$$k \min_{0 \leq i \leq k-1} G_i \leq \sum_{i=0}^{k-1} G_i \leq \mathcal{E}_0.$$

For the averaged iterate, convexity of F gives

$$F(\bar{v}_k) = F\left(\frac{1}{k} \sum_{i=0}^{k-1} v_i\right) \leq \frac{1}{k} \sum_{i=0}^{k-1} F(v_i).$$

Thus

$$F(\bar{v}_k) - F^* \leq \frac{1}{k} \sum_{i=0}^{k-1} (F(v_i) - F^*) \leq \frac{\mathcal{E}_0}{k}.$$

Finally, since the nonnegative series $\sum_{i=0}^{\infty} G_i$ is bounded by \mathcal{E}_0 , we have $G_k \rightarrow 0$, that is, $F(v_k) \rightarrow F^*$. \square

Remark 5. The theorem gives an $O(1/k)$ rate for the best iterate and for the averaged iterate. It does not claim an $O(1/k)$ rate for the last iterate v_k . The descent inequality implies $F(v_k) \rightarrow F^*$, but a last-iterate rate would require an additional argument, for instance a monotonicity property or a sharper control of the objective gaps.

4. Numerical tests

We test Prox-NAG-GS on four composite optimization benchmarks and one additional diagnostic experiment. The main benchmarks are intended to evaluate the practical behavior of the method. The deterministic tests use Elastic Net and Group Lasso objectives. The stochastic tests use softmax regression on MNIST, with either an entrywise ℓ_1 penalty or a Group Lasso penalty. These tests are intended to check two points: whether the proximal extension keeps the fast behavior observed for NAG-GS in deterministic problems, and how it behaves in stochastic learning when the nonsmooth term promotes sparsity.

In addition to these performance-oriented tests, we include a separate deterministic check of the theoretical regime. In the convergence proof, the algorithmic curvature parameter is required to satisfy the sufficient condition $\hat{\mu} \geq L$. In the main numerical comparisons, however, $\hat{\mu}$ is tuned empirically. The purpose of the additional test is therefore not to improve the best performance, but to verify that the conservative regime covered by the theory is numerically meaningful. We run Prox-NAG-GS with $\hat{\mu} = L$, monitor the objective gaps at both x_k and v_k , and record the augmented Lyapunov quantity used in Theorem 1.

All results are averaged over five random seeds. In the main performance benchmarks, all methods are tuned with Optuna [1], using the same tuning budget inside each benchmark. In the deterministic tests, the tuning criterion is based on the optimality gap. In the stochastic tests, the tuning criterion is based on validation performance. After each epoch, we evaluate the full regularized objective on the whole training set. Moreover, in all plots, solid curves show averages over five seeds, and shaded regions show one standard deviation.

For deterministic problems, we report the optimality gap $F(x_k) - F^*$, where F^* is computed by a high-precision reference solver. Note that for Prox-NAG-GS, the deterministic performance plots report the objective value at x_k , which is the practical output iterate in our implementation. The theory is stated for v_k , the proximal variable used in the Lyapunov analysis. At a fixed point of the deterministic iteration, the two variables coincide. In the additional theory-regime test, we report both $F(x_k) - F^*$ and $F(v_k) - F^*$, precisely to connect the numerical output with the variable used in the proof. For stochastic problems, we report the full objective, the data-fit term, the regularization term, test accuracy, sparsity, and wall-clock time. All experiments were run on Google Colab using an A100 GPU. The code used to generate all tables and figures is publicly available; see the reproducibility paragraph at the end of this section.

4.1. Deterministic Elastic Net

The first deterministic benchmark is the Elastic Net problem

$$\min_{x \in \mathbb{R}^d} \frac{1}{2} \|Ax - b\|_2^2 + \frac{\lambda_2}{2} \|x\|_2^2 + \lambda_1 \|x\|_1. \quad (33)$$

We compare Prox-NAG-GS with ISTA [11], FISTA [5], and Chambolle-Pock [7]. We use two instances. In the first one, A is generated as a Gaussian random matrix. In the second one, A is a synthetic random matrix with controlled condition number close to 10^3 . We refer to the two instances as the easy and hard cases, respectively.

Table 1. Deterministic Elastic Net. Final objective, iterations to reach the 10^{-6} optimality gap, and wall-clock time. Values are averages over five seeds.

Instance	Method	Final obj.	Iterations to 10^{-6}	Time (s)
Easy	ISTA	4.1050	95.4	0.1183
Easy	FISTA	4.1050	68.4	0.1163
Easy	Chambolle-Pock	4.1050	67.4	0.1016
Easy	Prox-NAG-GS	4.1050	28.0	0.1220
Hard	ISTA	0.6798	100.0	0.1976
Hard	FISTA	0.6798	61.6	0.1897
Hard	Chambolle-Pock	0.6798	93.6	0.2063
Hard	Prox-NAG-GS	0.6798	24.4	0.2131

Table 1 shows that Prox-NAG-GS reaches the same final objective as the baselines while requiring substantially fewer iterations. At the 10^{-6} gap threshold, the iteration reduction ranges from $2.41\times$ to $3.41\times$ on the easy instance and from $2.52\times$ to $4.10\times$ on the hard instance.

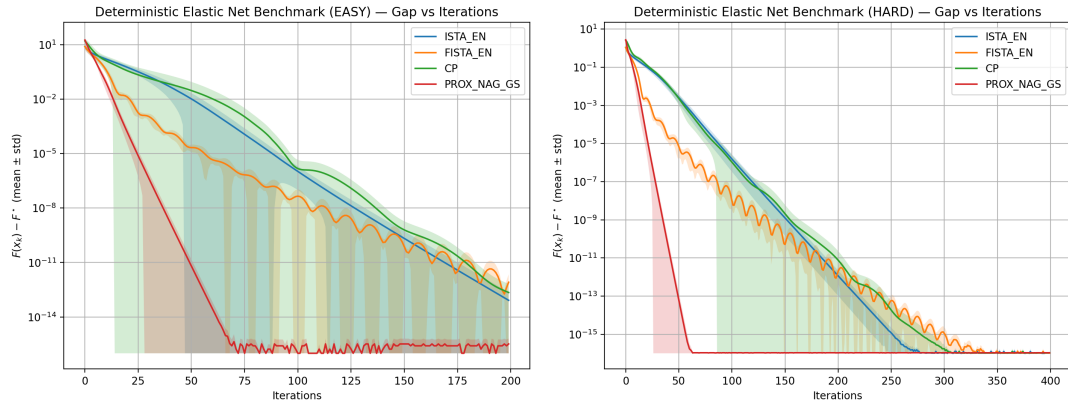


Figure 1. Deterministic Elastic Net. Optimality gap $F(x_k) - F^*$ versus iterations. Left: easy instance. Right: hard instance.

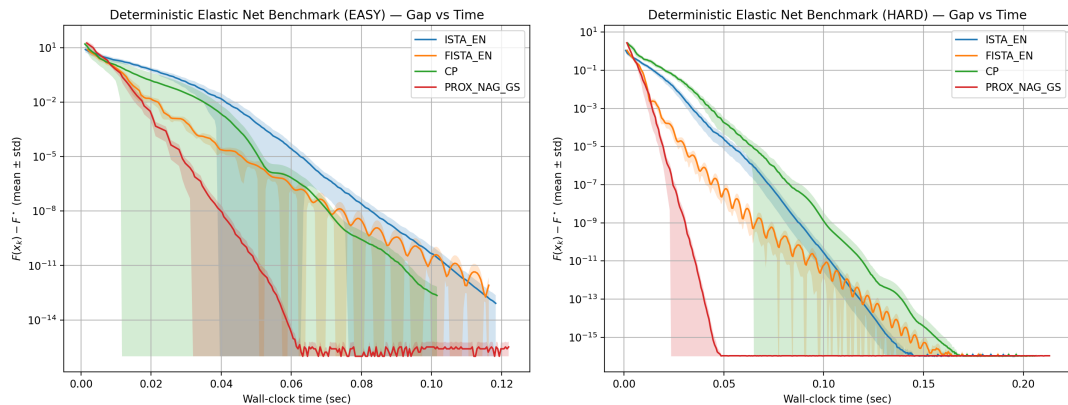


Figure 2. Deterministic Elastic Net. Optimality gap $F(x_k) - F^*$ versus wall-clock time. Left: easy instance. Right: hard instance.

All methods reach the same final objective up to the reported precision. Prox-NAG-GS reaches the 10^{-6} gap threshold with substantially fewer iterations. On the easy instance, the iteration reduction ranges from $2.41\times$ to $3.41\times$, depending on the baseline. On the hard instance, where the synthetic matrix has condition number close to 10^3 , it ranges from $2.52\times$ to $4.10\times$.

The wall-clock comparison is less favorable in this benchmark. Although Prox-NAG-GS needs fewer iterations, one iteration is slightly more expensive in the present implementation. Hence, the Elastic Net experiment mainly shows an iteration-efficiency advantage, rather than a clear runtime advantage.

4.2. Deterministic Group Lasso

We next consider the Group Lasso problem

$$\min_{x \in \mathbb{R}^d} \frac{1}{2} \|Ax - b\|_2^2 + \frac{\lambda_2}{2} \|x\|_2^2 + \lambda_g \sum_{G \in \mathcal{G}} \|x_G\|_2. \quad (34)$$

The groups are contiguous blocks of size 10. The ground truth contains 8 active groups. This benchmark tests whether the proximal NAG-GS update remains effective for a structured nonsmooth penalty.

Table 2. Deterministic Group Lasso. Final objective, active groups, iterations to reach the 10^{-6} optimality gap, and wall-clock time. Values are averages over five seeds.

Instance	Method	Final obj.	Active groups	Iter. to 10^{-6}	Time (s)
Easy	Group-ISTA	5.6159	8.0	125.8	0.2302
Easy	Group-FISTA	5.6159	8.0	93.2	0.2250
Easy	Group-CP	5.6159	8.0	69.0	0.2304
Easy	Group Prox-NAG-GS	5.6159	8.0	34.0	0.1846
Hard	Group-ISTA	0.9366	9.0	161.6	0.4215
Hard	Group-FISTA	0.9366	9.0	88.6	0.4225
Hard	Group-CP	0.9366	9.0	140.4	0.4220
Hard	Group Prox-NAG-GS	0.9366	9.0	30.8	0.3768

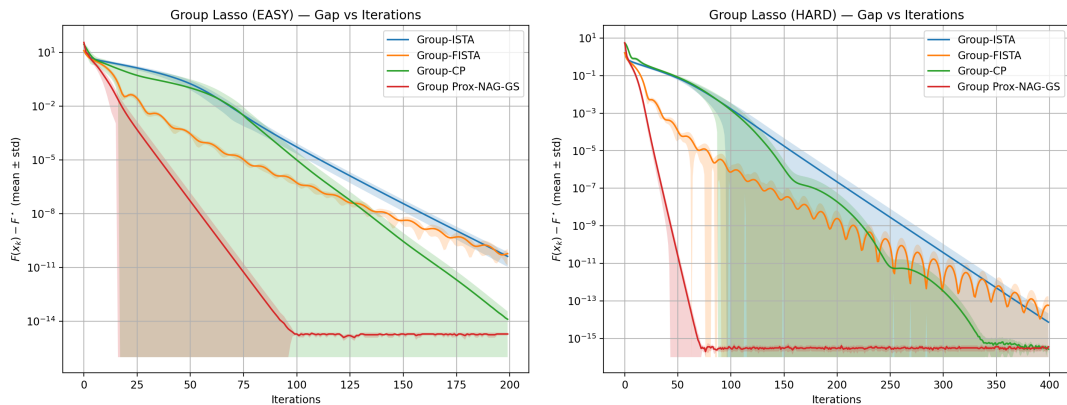


Figure 3. Deterministic Group Lasso. Optimalty gap $F(x_k) - F^*$ versus iterations. Left: easy instance. Right: hard instance.

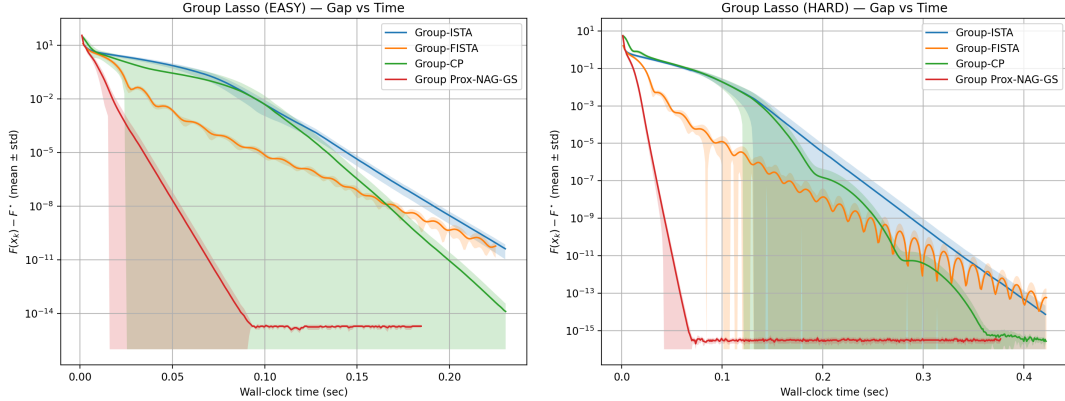


Figure 4. Deterministic Group Lasso. Optimalty gap $F(x_k) - F^*$ versus wall-clock time. Left: easy instance. Right: hard instance.

This benchmark gives the clearest deterministic evidence in favor of Prox-NAG-GS. All methods reach the same objective value and recover the same number of active groups. However, Prox-NAG-GS reaches the 10^{-6} gap threshold in significantly fewer iterations. In contrast with the Elastic Net test, this also translates into the best wall-clock time on both the easy and the hard instances.

4.3. Numerical check of the theoretical regime

The previous deterministic tests use tuned parameters and are meant to compare Prox-NAG-GS with standard proximal baselines. We now perform a different experiment. Its goal is to check the parameter regime used in the convergence proof. More precisely, we run Prox-NAG-GS on the deterministic Elastic Net problem with

$$\hat{\mu} = L,$$

where L is the smoothness constant of the differentiable part. This is the boundary case of the sufficient condition $\hat{\mu} \geq L$ used in Theorem 1.

This experiment is not intended as a performance comparison. The tuned values of $\hat{\mu}$ used in the main benchmarks can be more aggressive than the conservative value covered by the theorem. The purpose here is instead to verify that the theoretical regime gives the behavior predicted by the analysis.

Figure 5 reports the results. The left panel shows the objective gaps at both variables. The gap at v_k is the one directly connected to the Lyapunov analysis, while x_k is the practical output variable used in the deterministic experiments. Both gaps decrease steadily, and the two curves become almost indistinguishable after a short initial phase. This is consistent with the fact that x_k and v_k coincide at a fixed point of the deterministic iteration.

The right panel reports the augmented Lyapunov quantity

$$\mathcal{L}_k = F(v_k) - F^* + b \|v_k - x^*\|^2 + c \|x_k - x^*\|^2.$$

It decreases along the iterations and remains below the theoretical envelope $\mathcal{L}_0 \theta^k$. For each seed, we also checked the contraction inequality

$$\mathcal{L}_{k+1} \leq \theta \mathcal{L}_k,$$

where θ is the value given by Theorem 1. No violation was observed in the five runs. Finally, the mismatch-absorption term from Lemma 6 remained nonpositive up to numerical precision for all iterations and all seeds. This gives a direct numerical check that the conservative condition $\hat{\mu} \geq L$ leads to the behavior predicted by the proof.

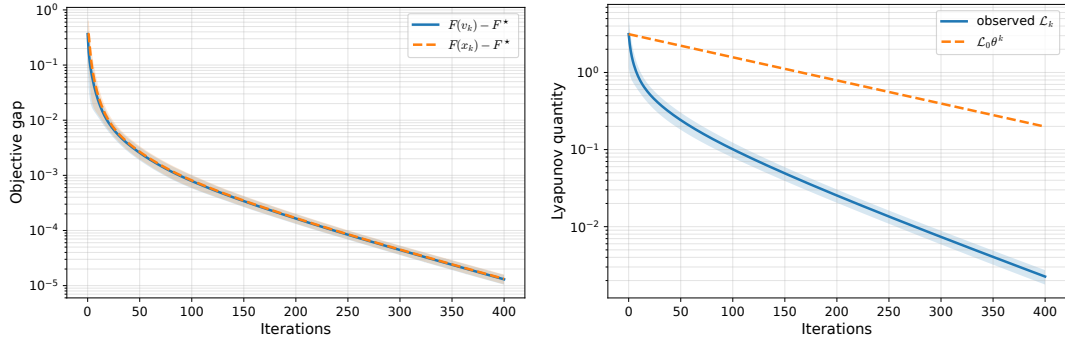


Figure 5. Numerical check of the theoretical regime on the deterministic Elastic Net benchmark with $\hat{\mu} = L$. Left: objective gaps at x_k and v_k . Right: augmented Lyapunov quantity \mathcal{L}_k compared with the theoretical envelope $\mathcal{L}_0 \theta^k$. Curves are averaged over five seeds, and shaded regions show one standard deviation.

4.4. Stochastic ℓ_1 softmax regression

The stochastic ℓ_1 benchmark uses softmax regression on MNIST:

$$\min_{W \in \mathbb{R}^{d \times c}} \frac{1}{n} \sum_{i=1}^n \ell_i(W) + \lambda_1 \|W\|_1 + \frac{\lambda_2}{2} \|W\|_F^2. \quad (35)$$

We compare Prox-NAG-GS with Prox-SGD. Both methods use the same mini-batch size and the same train-validation-test split for each seed.

Table 3. Stochastic ℓ_1 softmax regression. Mean \pm standard deviation over five seeds.

Method	Final obj.	Data-fit	Reg. term	Test acc.	Sparsity	Time (s)
Prox-SGD	0.3362 \pm 0.0008	0.2802 \pm 0.0007	0.0561 \pm 0.0002	0.9206 \pm 0.0008	0.4127 \pm 0.0035	37.53 \pm 0.68
Prox-NAG-GS	0.3351 \pm 0.0049	0.2723 \pm 0.0025	0.0628 \pm 0.0027	0.9212 \pm 0.0017	0.3402 \pm 0.0247	37.92 \pm 0.32

Table 4. λ_1 sweep for stochastic ℓ_1 softmax regression. Values are averages over five seeds.

λ_1	Method	Final test acc.	Best-val test acc.	Sparsity
10^{-4}	Prox-SGD	0.92056	0.92090	0.41268
10^{-4}	Prox-NAG-GS	0.92124	0.92144	0.34015
5×10^{-4}	Prox-SGD	0.90966	0.91020	0.54074
5×10^{-4}	Prox-NAG-GS	0.90854	0.91110	0.38997
10^{-3}	Prox-SGD	0.89938	0.90070	0.62401
10^{-3}	Prox-NAG-GS	0.89994	0.90558	0.43020
5×10^{-3}	Prox-SGD	0.85334	0.85752	0.83151
5×10^{-3}	Prox-NAG-GS	0.58604	0.88084	0.45298

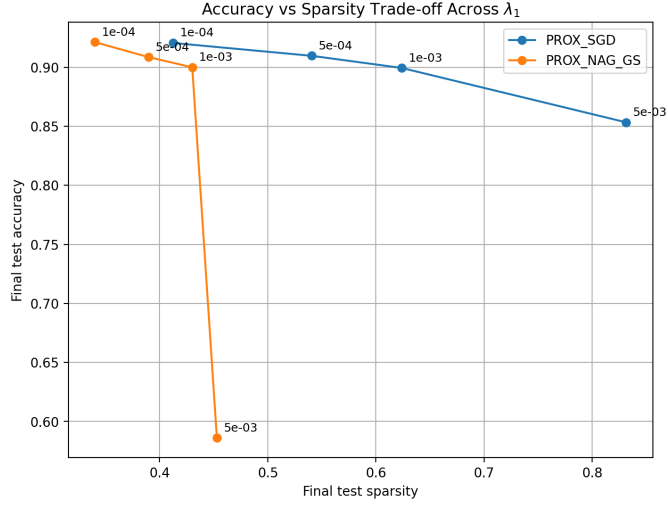


Figure 6. Stochastic ℓ_1 softmax regression. Accuracy-sparsity trade-off across different values of λ_1 .

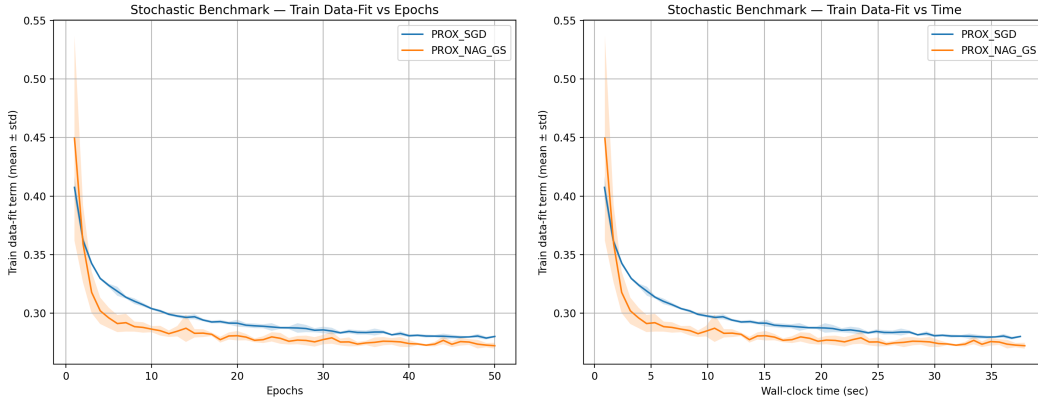


Figure 7. Stochastic ℓ_1 softmax regression. Training data-fit term versus epochs and wall-clock time.

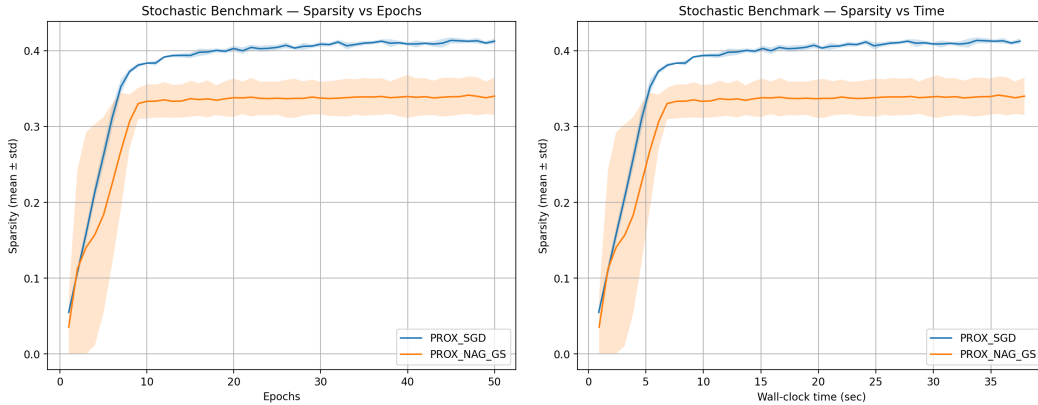


Figure 8. Stochastic ℓ_1 softmax regression. Sparsity versus epochs and wall-clock time.

The stochastic ℓ_1 experiment complements the deterministic tests. Prox-NAG-GS obtains a slightly lower full objective and a lower data-fit term for the base value of λ_1 , with essentially the same test accuracy. However, Prox-SGD gives a smaller

regularization term and produces a sparser model.

The sweep over λ_1 confirms this trade-off. For small and moderate regularization, Prox-NAG-GS remains competitive in accuracy, but it produces denser solutions. For the largest value of λ_1 , the final iterate of Prox-NAG-GS becomes less stable: the final test accuracy drops, even though the best validation checkpoint remains competitive. This suggests that, in the strongly regularized stochastic regime, the present version of Prox-NAG-GS may need additional stabilization, for instance damping, averaging, or restart strategies.

4.5. Stochastic Group Lasso

The stochastic Group Lasso benchmark also uses softmax regression on MNIST. We define one group per input pixel, grouping the weights associated with this pixel across all output classes:

$$\min_W \frac{1}{n} \sum_{i=1}^n \ell_i(W) + \lambda_g \sum_{G \in \mathcal{G}} \|W_G\|_2 + \frac{\lambda_2}{2} \|W\|_F^2. \quad (36)$$

The model has 784 groups, each of size 10.

Table 5. Stochastic Group Lasso on MNIST softmax regression. Mean \pm standard deviation over five seeds.

Method	Final obj.	Data-fit	Reg. term	Test acc.	Group sparsity	Time (s)
Group Prox-SGD	0.2983 \pm 0.0010	0.2668 \pm 0.0011	0.0315 \pm 0.0003	0.9229 \pm 0.0007	0.2566 \pm 0.0098	615.83 \pm 11.40
Group Prox-NAG-GS	0.3061 \pm 0.0140	0.2637 \pm 0.0109	0.0424 \pm 0.0040	0.9200 \pm 0.0066	0.1852 \pm 0.0272	612.42 \pm 13.34

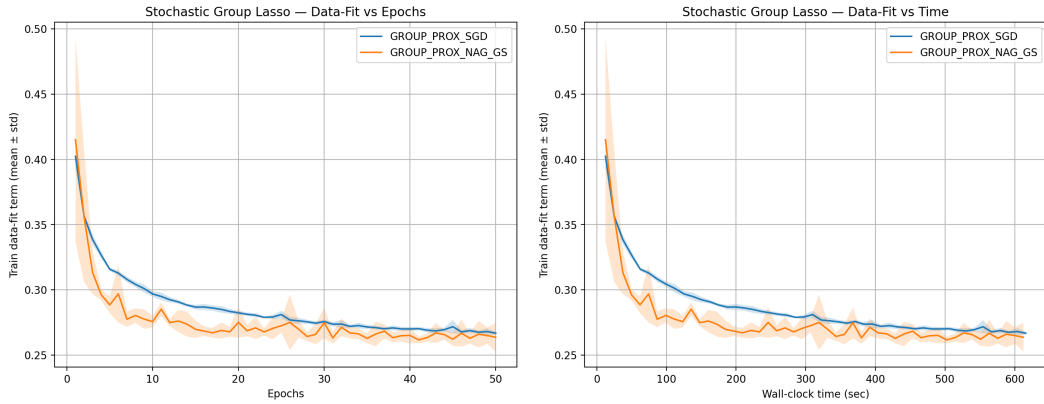


Figure 9. Stochastic Group Lasso. Training data-fit term versus epochs and wall-clock time.

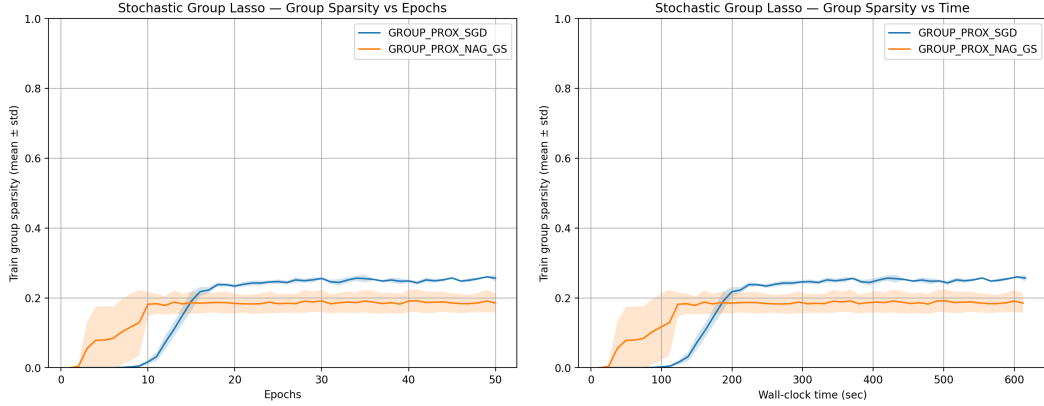


Figure 10. Stochastic Group Lasso. Group sparsity versus epochs and wall-clock time.

The stochastic Group Lasso experiment is consistent with the stochastic ℓ_1 test. Group Prox-NAG-GS gives the lowest data-fit term, while Group Prox-SGD gives the lowest full regularized objective. The reason is again the regularization term: Prox-SGD produces stronger group sparsity, whereas Prox-NAG-GS keeps denser weights. The test accuracies are close, with a small advantage for Prox-SGD at the final iterate. The wall-clock times are comparable.

4.6. Discussion of the experiments

The deterministic experiments support the proximal extension clearly. On both Elastic Net and Group Lasso, Prox-NAG-GS reaches the same objective value as the baselines and needs fewer iterations. The strongest deterministic result is obtained on the Group Lasso benchmark, where the iteration advantage also leads to the best wall-clock time.

The stochastic experiments also show competitive behavior. Prox-NAG-GS compares favorably with Prox-SGD in terms of data-fit reduction and gives similar test accuracies. In both stochastic benchmarks, the method tends to decrease the smooth empirical loss more strongly. At the same time, the experiments reveal a different regularization behavior. Prox-SGD usually produces sparser models and may give a lower full regularized objective when the nonsmooth regularization is large.

Overall, the experiments suggest that the semi-implicit proximal coupling is useful in deterministic composite problems, especially when the proximal operator is structured but still cheap to compute. They also suggest that Prox-NAG-GS is promising in stochastic composite learning, but that its regularization behavior may need more careful damping, averaging, or restart strategies.

4.6.0.1. Reproducibility and runtime.. The full Python code, including the scripts used to regenerate the figures and tables reported in this section, is available at

<https://github.com/giselesikeh/prox-nag-gs-composite-optimization.git>.

The main experimental parameters are specified explicitly in the corresponding scripts, including the number of Optuna trials, the maximum number of iterations or epochs, the batch size, the MNIST train/validation/test split, the dimensions of the deterministic problems, and the values of $\lambda_1, \lambda_2, \lambda_g$. All experiments were run on Google Colab

using an A100 GPU. The reported times are wall-clock times measured in this environment. Absolute runtimes may differ on other hardware, but the repository contains the code and settings needed to reproduce the reported comparisons.

5. Conclusion

We introduced Prox-NAG-GS, a proximal extension of NAG-GS for composite optimization problems. The construction is direct: the second NAG-GS update can be written as the minimizer of a quadratic model, and adding the nonsmooth term to this model gives a proximal update. The method therefore keeps the semi-implicit coupling of NAG-GS while allowing nonsmooth regularizers and simple convex constraints to be handled through their proximal operators.

We also provided deterministic convergence guarantees. The main point in the analysis is that the gradient is evaluated at x_{k+1} , while the proximal step returns v_{k+1} . This creates a mismatch that does not appear in the standard proximal-gradient proof. Under the sufficient condition $\hat{\mu} \geq L$, this term can be controlled. In the strongly convex composite case, we prove a linear convergence result using an augmented Lyapunov function involving both $\|v_k - x^*\|^2$ and $\|x_k - x^*\|^2$. We also showed that the same Lyapunov structure gives an $O(1/k)$ rate for the best iterate and for the averaged iterate in the convex case. These results do not claim optimal accelerated rates, but they provide a rigorous convergence analysis for the proximal version of NAG-GS.

The deterministic experiments support the method. On Elastic Net and Group Lasso benchmarks, Prox-NAG-GS reaches the same objective values as ISTA, FISTA and Chambolle-Pock, while requiring fewer iterations. The Group Lasso experiment gives the strongest deterministic evidence: Prox-NAG-GS is faster both in iterations and in wall-clock time. The stochastic experiments also show competitive behavior. Prox-NAG-GS compares favorably with Prox-SGD in terms of data-fit reduction and gives similar test accuracies. At the same time, the experiments reveal a different regularization behavior: Prox-SGD usually produces sparser solutions and may give a lower full regularized objective when the nonsmooth regularization is large. This suggests that Prox-NAG-GS is promising in stochastic composite learning, but that its regularization behavior may need more careful damping, averaging, or restart strategies.

Several questions remain open. The condition $\hat{\mu} \geq L$ used in the proof is conservative and does not cover all parameter choices that work well in practice. A sharper analysis could explain larger effective stepsizes and possibly lead to accelerated rates. Another natural direction is the stochastic analysis of Prox-NAG-GS, especially under mini-batch gradients and variance assumptions. Finally, broader numerical tests on larger-scale learning problems would help clarify when the semi-implicit proximal coupling is most beneficial.

References

- [1] T. Akiba, S. Sano, T. Yanase, T. Ohta, and M. Koyama, *Optuna: A Next-generation Hyperparameter Optimization Framework*, in *Proceedings of the 25th ACM SIGKDD International Conference on Knowledge Discovery & Data Mining*. 2019, pp. 2623–2631.
- [2] F. Alvarez and H. Attouch, *An inertial proximal method for maximal monotone operators via discretization of a nonlinear oscillator with damping*, *Set-Valued Analysis* 9 (2001), pp. 3–11.

- [3] H. Attouch, Z. Chbani, and H. Riahi, *Fast proximal methods via time scaling of damped inertial dynamics*, SIAM Journal on Optimization 29 (2019), pp. 2227–2256.
- [4] H.H. Bauschke and P.L. Combettes, *Convex Analysis and Monotone Operator Theory in Hilbert Spaces*, 2nd ed., Springer, 2017.
- [5] A. Beck and M. Teboulle, *A fast iterative shrinkage-thresholding algorithm for linear inverse problems*, SIAM Journal on Imaging Sciences 2 (2009), pp. 183–202.
- [6] L. Bottou, F.E. Curtis, and J. Nocedal, *Optimization methods for large-scale machine learning*, SIAM Review 60 (2018), pp. 223–311.
- [7] A. Chambolle and T. Pock, *A first-order primal-dual algorithm for convex problems with applications to imaging*, Journal of Mathematical Imaging and Vision 40 (2011), pp. 120–145.
- [8] P.L. Combettes and J.C. Pesquet, *Proximal splitting methods in signal processing*, in *Fixed-Point Algorithms for Inverse Problems in Science and Engineering*, Springer, 2011, pp. 185–212.
- [9] P.L. Combettes and V.R. Wajs, *Signal recovery by proximal forward-backward splitting*, Multiscale Modeling & Simulation 4 (2005), pp. 1168–1200.
- [10] L. Condat, *A primal-dual splitting method for convex optimization involving lipschitzian, proximable and linear composite terms*, Journal of Optimization Theory and Applications 158 (2013), pp. 460–479.
- [11] I. Daubechies, M. Defrise, and C. De Mol, *An iterative thresholding algorithm for linear inverse problems with a sparsity constraint*, Communications on Pure and Applied Mathematics 57 (2004), pp. 1413–1457.
- [12] A. Defazio, F. Bach, and S. Lacoste-Julien, *SAGA: A fast incremental gradient method with support for non-strongly convex composite objectives*, in *Advances in Neural Information Processing Systems*, Vol. 27. 2014, pp. 1646–1654.
- [13] J. Duchi and Y. Singer, *Efficient online and batch learning using forward backward splitting*, Journal of Machine Learning Research 10 (2009), pp. 2899–2934.
- [14] S. Ghadimi and G. Lan, *Stochastic first- and zeroth-order methods for nonconvex stochastic programming*, SIAM Journal on Optimization 23 (2013), pp. 2341–2368.
- [15] S. Ghadimi, G. Lan, and H. Zhang, *Mini-batch stochastic approximation methods for nonconvex stochastic composite optimization*, Mathematical Programming 155 (2016), pp. 267–305.
- [16] R. Johnson and T. Zhang, *Accelerating stochastic gradient descent using predictive variance reduction*, in *Advances in Neural Information Processing Systems*, Vol. 26. 2013, pp. 315–323.
- [17] G. Lan, *An optimal method for stochastic composite optimization*, Mathematical Programming 133 (2012), pp. 365–397.
- [18] V. Leplat, D. Merkulov, A. Katrutsa, D. Bershatsky, O. Tsymboi, and I. Oseledets, *NAG-GS: Semi-implicit, accelerated and robust stochastic optimizer*, arXiv preprint arXiv:2209.14937 (2022).
- [19] A. Moudafi and M. Oliny, *Convergence of a splitting inertial proximal method for monotone operators*, Journal of Computational and Applied Mathematics 155 (2003), pp. 447–454.
- [20] Y. Nesterov, *A method for solving the convex programming problem with convergence rate $O(1/k^2)$* , in *Soviet Mathematics Doklady*, Vol. 27. 1983, pp. 372–376.
- [21] Y. Nesterov, *Gradient methods for minimizing composite functions*, Mathematical Programming 140 (2013), pp. 125–161.
- [22] Y. Nesterov, *Lectures on Convex Optimization*, Springer, 2018.
- [23] P. Ochs, Y. Chen, T. Brox, and T. Pock, *iPiano: Inertial proximal algorithm for nonconvex optimization*, SIAM Journal on Imaging Sciences 7 (2014), pp. 1388–1419.
- [24] N. Parikh and S. Boyd, *Proximal algorithms*, Foundations and Trends in Optimization 1 (2014), pp. 127–239.
- [25] B.T. Polyak, *Some methods of speeding up the convergence of iteration methods*, USSR Computational Mathematics and Mathematical Physics 4 (1964), pp. 1–17.

- [26] M. Schmidt, N. Le Roux, and F. Bach, *Minimizing finite sums with the stochastic average gradient*, *Mathematical Programming* 162 (2017), pp. 83–112.
- [27] W. Su, S. Boyd, and E.J. Candès, *A differential equation for modeling Nesterov’s accelerated gradient method: Theory and insights*, *Journal of Machine Learning Research* 17 (2016), pp. 1–43.
- [28] P. Tseng, *On accelerated proximal gradient methods for convex-concave optimization*, *Manuscript* (2008). May 2008.
- [29] B.C. Vu, *A splitting algorithm for dual monotone inclusions involving cocoercive operators*, *Advances in Computational Mathematics* 38 (2013), pp. 667–681.
- [30] A.C. Wilson, B. Recht, and M.I. Jordan, *A lyapunov analysis of accelerated methods in optimization*, *Journal of Machine Learning Research* 22 (2021), pp. 1–34.
- [31] L. Xiao, *Dual averaging methods for regularized stochastic learning and online optimization*, *Journal of Machine Learning Research* 11 (2010), pp. 2543–2596.
- [32] L. Xiao and T. Zhang, *A proximal stochastic gradient method with progressive variance reduction*, *SIAM Journal on Optimization* 24 (2014), pp. 2057–2075.